



Get Clarity On Generics

Cost-Effective CT & MRI Contrast Agents



FRESENIUS
KABI

WATCH VIDEO

AJNR

The detection of intracranial calcifications by MR.

R F Oot, P F New, J Pile-Spellman, B R Rosen, G M Shoukimas
and K R Davis

AJNR Am J Neuroradiol 1986, 7 (5) 801-809

<http://www.ajnr.org/content/7/5/801>

This information is current as
of August 14, 2025.

The Detection of Intracranial Calcifications by MR

Robert F. Oot¹
 Paul F. J. New
 John Pile-Spellman
 Bruce R. Rosen
 Gregory M. Shoukimas
 Kenneth R. Davis

Twenty patients in whom CT had unequivocally demonstrated the presence of calcification in a diversity of lesions and who had undergone MR, performed at 0.6 T and with standard T1- and T2-weighted pulse sequences, were retrospectively studied to determine the MR signal-intensity characteristics of the calcifications and to assess the ability of MR to detect the presence of this abnormality. CT proved superior to MR in detecting and characterizing calcification. In seven of 20 cases, the apparent extent of calcification was equal by both imaging techniques, and in 13 of the 20 cases, CT showed more extensive abnormality. In five of the 20 cases, the calcifications were seen by MR as regions of profoundly reduced signal intensity, approximately equal to cortical bone, in all pulse sequences. In 12 of the 20 cases, the signal intensity was profoundly reduced in one or more, but not all, pulse sequences. T2-weighted pulse sequences were most sensitive in detecting calcification of signal void. Reviewed without knowledge of the CT findings, the MR images were interpreted as definitely indicative of the presence of calcification in three of the 20 cases. In seven of the 20 cases, the MR images raised the possibility of calcification but were less definitive than the CT findings. In 10 of the 20 cases, MR was judged indeterminate for the presence of calcification.

It is axiomatic that determining the presence, location, distribution, and texture of intracranial calcification is of major importance in radiologic and differential diagnoses. CT has proved to be highly sensitive in detecting calcification [1] and is currently the standard against which other techniques must be measured. Numerous reports comparing the relative effectiveness of MR and CT in evaluating a broad spectrum of intracranial diseases have been published [2-15], yet the relative capability of MR to provide reliable evidence of intracranial calcification has received little direct attention. While a number of workers have noted difficulty in recognizing calcification with reliability in the MR image [4, 8, 9, 12-15], only one recent report has specifically addressed this issue [16]. Because of the major importance of this finding in neurodiagnosis, we retrospectively analyzed and compared the effectiveness of MR in detecting calcification in 20 patients in whom CT very clearly demonstrated its presence in a diversity of lesions.

Subjects and Methods

Twenty patients were retrospectively selected on the basis of definite demonstration of abnormal calcification by CT in a variety of disease processes. A patient with extremely dense normal calcification of the glomi of the choroid plexi was also included in this study. The patients included 11 males and nine females, ranging in age from 4 to 64 years. Individual patient data are summarized in Table 1. The diagnoses were suggested by CT in all patients and were confirmed histologically in 11 instances. Angiography confirmed the diagnosis in cases of arteriovenous malformation (patients 3 and 19) and aneurysm (patient 1). In those patients treated conservatively, the diagnoses were based on clinical and CT findings.

Calcification was punctate in one case, 11 calcifications were between 2.5 and 7.5 mm,

Received January 2, 1986; accepted after revision April 7, 1986.

Presented at the annual meeting of the American Society of Neuroradiology, San Diego, January 1986.

¹ All authors: Department of Radiology, Massachusetts General Hospital and the Harvard Medical School, Boston, MA 02114. Address reprint requests to R. F. Oot, Section of Neuroradiology, Massachusetts General Hospital, 32 Fruit St., Boston, MA 02114.

AJNR 7:801-809, September/October 1986
 0195-6108/86/0705-0801

© American Society of Neuroradiology

TABLE 1: Summary of Patient Data

Case No.	Diagnosis	Location	Size ¹ and Attenuation Coefficient of Calcification	Detectability on MR ²
1	Aneurysm	R. parasellar	M, 185	I
2	Meningioma	Foramen magnum	M, 225	D
3	Arteriovenous malformation	L. basal ganglia	M, 125	P
4	Meningioma	L. lateral ventricle	L, 765	D
5	Exostosis	L. temporal	L, 300	I
6	Chondrosarcoma	Suprasellar	L, 250	I
7	Astrocytoma (Grade II)	L. frontal	S, 75	I
8	Oligoastrocytoma	R. frontal	L, 350	I
9	Astrocytoma (Grade II)	Bifrontal, L. temporal	L, not available	I
10	Astrocytoma (Grade II)	Cerebellum	M, 175	I
11	Pineocytoma	Pineal	M, 250	P
12	Tuberose sclerosis	L. parietal	M, 105	P
13	Oligoastrocytoma	R. frontal	M, 130	I
14	Teratoma	Hypothalamus	M, 160	I
15	Craniopharyngioma	Suprasellar	M, 150	P
16	Normal choroid plexus	Lateral ventricle	L, 630	D
17	Meningioma	Third ventricle	L, 290	P
18	Undifferentiated pineal tumor	Pineal	L, 175	P
19	Arteriovenous malformation	L. cerebellum	M, 370	I
20	Calcified cyst	R. temporal	M, 450	P

¹ Size of calcification: S = small (<2.5 mm); M = medium (2.5–7.5 mm); L = large (>7.5 mm).

² Detectability: D = definitely calcified; P = probably calcified; I = indeterminate.

and eight were larger than 7.5 mm in maximum dimension. The CT scans were performed with third- and fourth-generation scanners, which included the GE 8800, GE 9800, and Siemens DR2. Section thickness was 10 mm in most cases. CT scans after IV contrast enhancement were performed in all patients, and unenhanced scans were available in 18 of 20 cases. Dense globular foci of calcification, with CT attenuation coefficients of 225 and 630 H, were present in the two cases in which unenhanced scans were not available (patients 2 and 16). The density of calcification was estimated in terms of CT attenuation and measured in Hounsfield units, as determined from the mean value of multiple region of interest (ROI) measurements, which were performed on unenhanced scans in all cases except patient 9.

MR was performed with a Technicare superconducting magnet operating at a field strength of 0.6 T and using the standard head coil and our routine pulse sequences. Pulse sequences included spin echo (SE), dual SE, and inversion recovery (IR). Almost all images were obtained in the axial plane and both T1- and T2-weighted sequences were performed in every patient. T1-weighted images were obtained with repetition times (TR) of 500–1000 msec and echo times (TE) of 30 msec; inversion recovery images were obtained with TRs of 1450–1650 msec, inversion time (TI) of 450–500 msec, and TEs of 30–32 msec. T2-weighted images were obtained with TRs of 1500–2000 msec and TEs of 60–120 msec. Images were acquired using 128 phase encoding (y-gradient) steps, interpolated to 256 for image display; 256 frequency encoding (x-gradient) steps were used for a total display matrix of 256 × 256. Transverse spatial resolution was 2.0 × 1.0 mm. All images were obtained with multislice technique and 7.5-mm section thickness except for patient 10, who was studied with a 2D single-slice technique with 8.0-mm thick sections.

The intracranial calcifications were identified, localized, and characterized by CT. Corresponding MR images were then reviewed in conjunction with the CT scans by three of the investigators to

determine the image characteristics of the calcifications. A grading scale was established on the basis of the signal intensity of the calcifications. The signal intensity of the calcifications was considered to be (1) profoundly reduced, if it approximated the level of cortical bone; (2) moderately reduced, if it was between cortical bone and cortical gray matter; or (3) within the range of contiguous soft tissues. The extent and morphology of the calcifications as depicted by MR and CT were compared. The MR studies were also reviewed by two investigators who had no knowledge of the CT findings specifically to assess the ability of MR to reliably predict the presence of calcification. On the basis of the MR images, the lesions were classified as being definitely calcified, probably calcified, or indeterminate with respect to the discrimination of this feature.

Results

The results of comparing the CT and MR images indicated that calcifications were seen as areas of profoundly reduced signal in all pulse sequences in five of 20 cases (Fig. 1). In 12 of 20 cases, the lesion demonstrated profoundly reduced signal in at least one, but not all, pulse sequences (Fig. 2). In one of 20 cases (patient 13), the signal intensity of the calcified region was in the range between cortical bone and gray matter on all pulse sequences. In two of 20 instances (patients 7 and 10), no corresponding area of reduced MR signal intensity was seen (Fig. 3).

The signal intensities of the calcifications and their relationship to pulse sequence are summarized in Table 2. Transverse-relaxation (T2) weighted pulse sequences were acquired in all patients and showed calcification as areas of

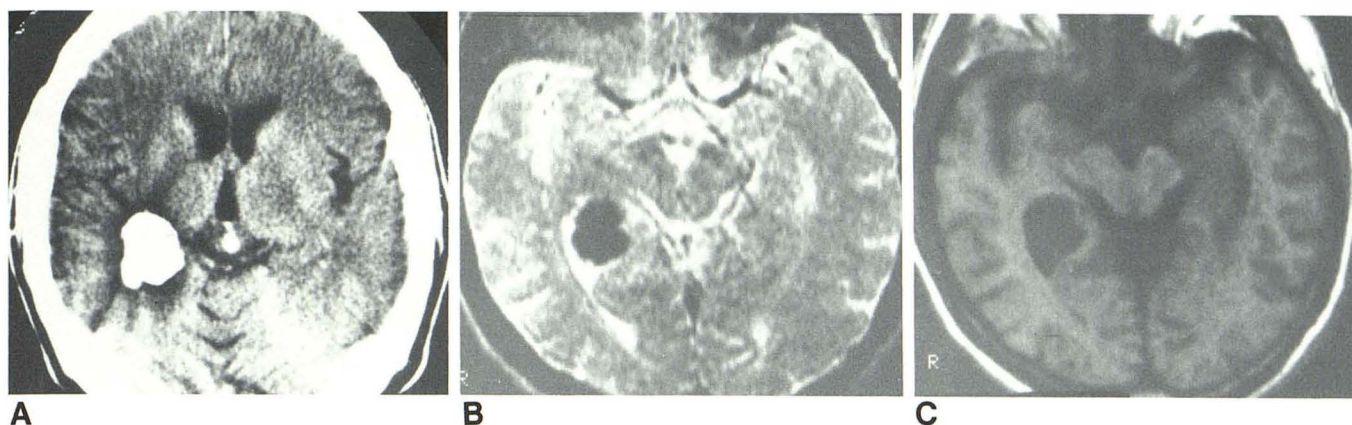


Fig. 1.—(Case 4) Intraventricular meningioma. **A**, Noncontrast CT. Densely calcified mass located in right lateral ventricle. **B**, SE 2000/(60)90, TR/TE, and **C**, IR 1500/450/32, TR/TI/TE. MR shows corresponding area of profound reduction in signal intensity.

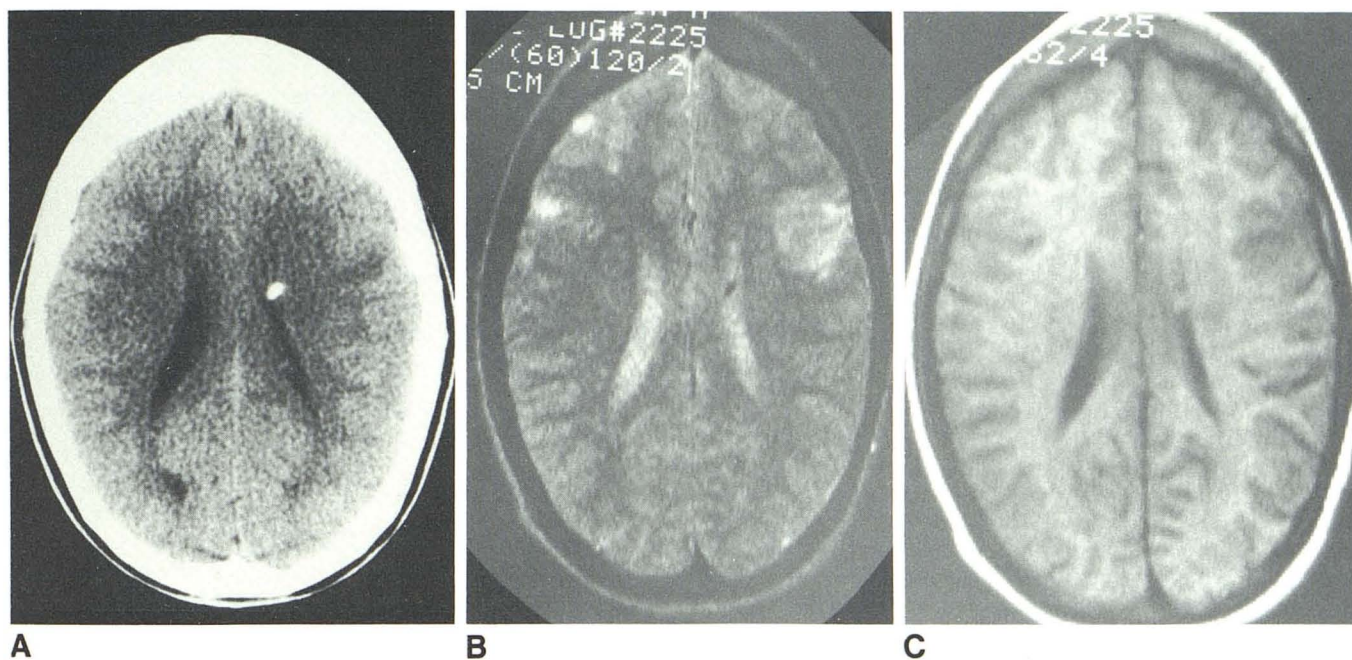


Fig. 2.—(Case 12) Tuberosclerosis. **A**, Noncontrast CT. Densely calcified periventricular abnormality. **B**, SE 2000/(60)120, TR/TE. Corresponding area of profoundly reduced signal intensity is shown on this T2-weighted image. **C**, IR 1500/450/32, TR/TI/TE. On this T1-weighted image the area of calcification

appears isosignal with white matter. The MR image in **B** depicts multiple additional areas of parenchymal abnormality, presumably cortical tubers, that were not detected by CT.

virtual signal void (signal intensity approximately equal to cortical bone), in 15 of 20 (75%) instances. In 16 cases, dual SE (2000/60,120) pulse sequences were used. In 10 of 16 cases, there was no appreciable change in the signal intensity of the calcifications relative to adjacent structures in comparing the 60- and 120-msec echo-delay images. In five of 16 cases, the signal intensity of the abnormality was relatively lower on the 60-msec image, and in one instance there was lower intensity on the 120-msec echo image. These changes in relative signal intensity were very subtle in all instances. IR

(1450–1500/450–500/30–32) sequences were obtained in 14 patients and T1-weighted SE (330–500/18–30) sequences were done in 10 cases. The calcifications were seen as areas of virtual signal void in six of 14 (43%) and three of 10 (30%) instances, respectively. Four patients had both T1-weighted SE and IR scans. In three instances, the calcifications showed no difference in signal intensity. In one patient (case 18), the calcification was seen as a virtual signal void on IR but had a signal intensity between cortical bone and cortical gray matter on the T1-weighted SE.

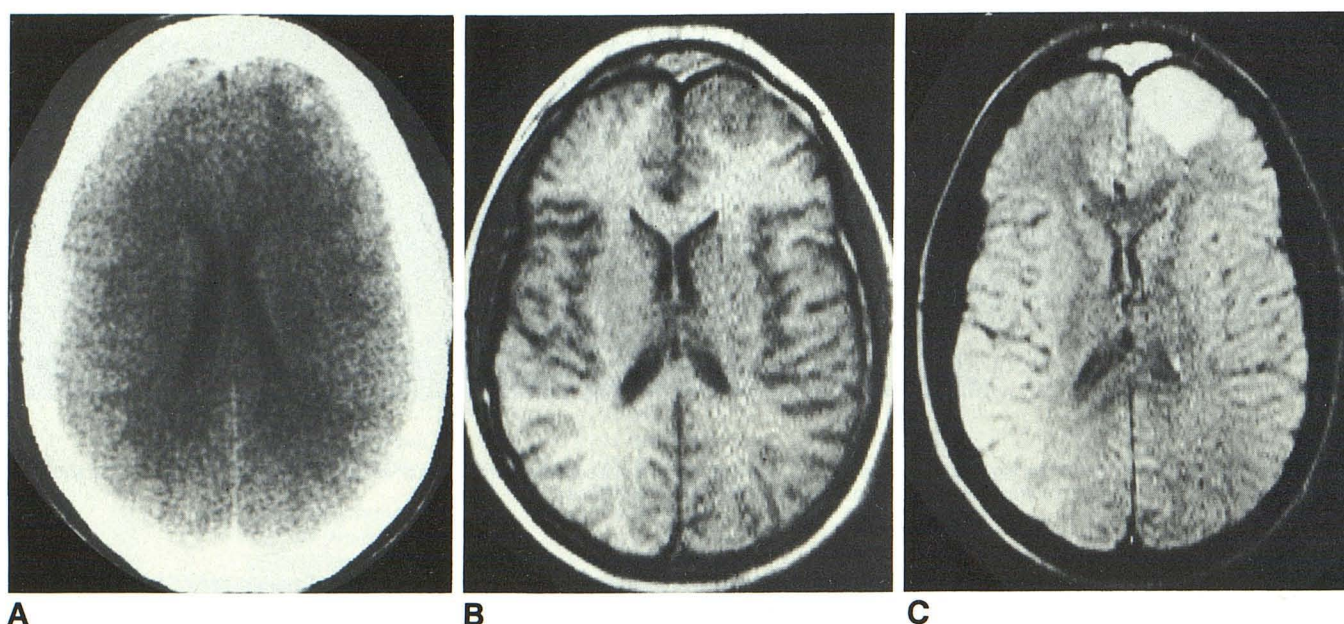


Fig. 3.—(Case 7) Astrocytoma, Grade II. **A**, Noncontrast CT. Punctate calcification present in left frontal lobe, surrounded by low density. **B**, IR 1500/450/32, TR/TI/TE. T1-weighted image shows the mass, characterized by

prolonged T1 relaxation time, but does not detect the calcification. **C**, SE 1500/60, TR/TE. T2-weighted image shows the abnormality has a prolonged T2 but, again, no area of decreased signal corresponding to the calcification is seen.

TABLE 2: MR Signal Intensity Characteristics of Intracranial Calcifications

Pulse Sequence	SI* Approx. Equal to Cortical Bone	SI* Between Cortical Bone and Cortical Gray Matter	SI* Within Range of Contiguous Soft Tissues
T1-weighted SE (500/30, 1000/30)	3/10	6/10	1/10
T2-weighted SE (2000/(60,120), 1500/60)	15/20	3/20	2/20
IR (1450–1650/450–500/30–32)	6/14	3/14	5/14

* SI = signal intensity.

In 13 of 20 cases, CT showed the calcifications to be more extensive than those seen on the MR images (Fig. 4), and in seven of 20 cases there was good correlation between the extent of abnormality depicted by each imaging technique. MR never showed more extensive calcification than that seen by CT. In all instances, CT provided more information about the morphology of the calcifications than did MR.

While no lesion entirely escaped detection by MR in our experience, in two patients, the lesions were more readily identified by CT but were much more subtly depicted by MR. One peripheral frontal lobe oligoastrocytoma (Fig. 5) and an exostosis arising from the petrous apex (Fig. 6) could potentially have escaped detection had only MR been performed.

Reviewed without knowledge of the CT findings, the MR images were interpreted as definitely indicating the presence of calcification in three of 20 cases. In seven of 20 cases, the MR images were interpreted as probably representing calci-

fication but were less definite than CT. In 10 of 20 cases, MR was judged to be indeterminate with respect to the presence of calcification. The latter group included some calcifications that were sufficiently large that partial volume averaging could not explain the lack of visualization on the MR images obtained with a slice thickness of 7.5 mm. The relationships between size and density of the calcifications and detectability are summarized in Tables 1 and 3.

Discussion

Calcification can occur in a wide range of conditions; Taveras and Wood [17] tabulate 49 causes, Newton and Potts [18] 44, and Harwood-Nash and Fitz [19] 59. The presence and morphologic features of this finding have a major influence on the likelihood of a specific diagnosis and may significantly influence patient management. CT has been shown to be

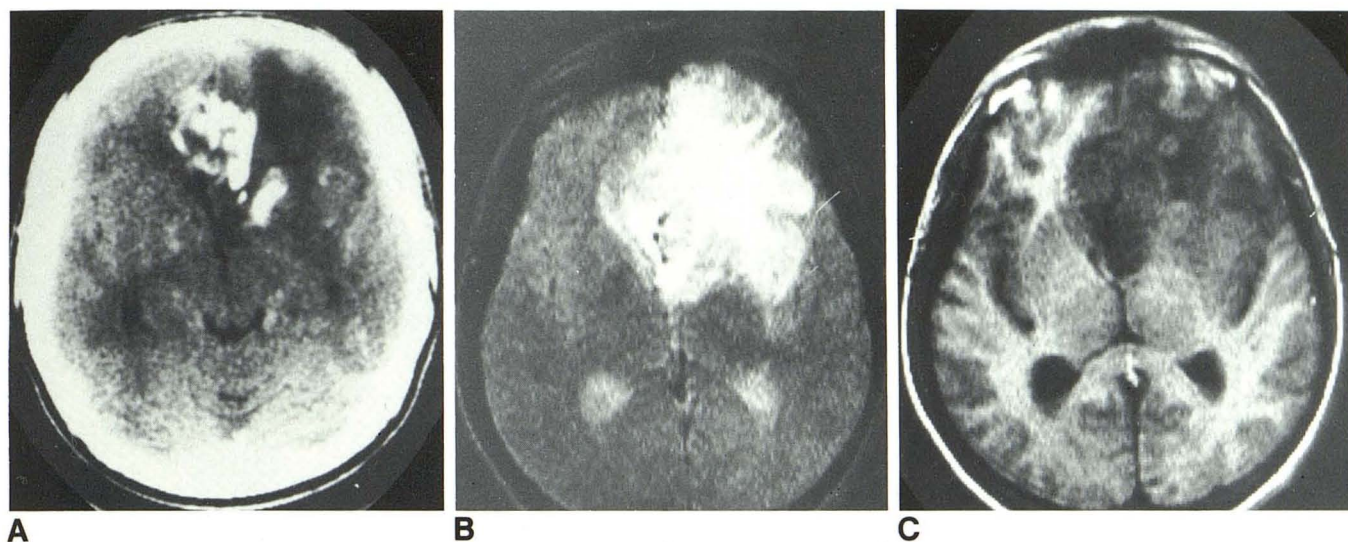


Fig. 4.—(Case 9) Astrocytoma, Grade II. **A**, Noncontrast CT. Extensive abnormality involving both frontal lobes, left temporal lobe, and basal ganglia. Multiple foci of dense calcification are seen. **B**, SE 2000/(60)120 TR/TE. T2-weighted image detects the extensive high-signal abnormality but fails to

accurately detect the calcifications. **C**, IR 1500/450/32, TR/T1/TE. T1-weighted image suggests calcifications, seen as areas of profoundly reduced signal intensity, but detects less of this abnormality than was shown by CT.

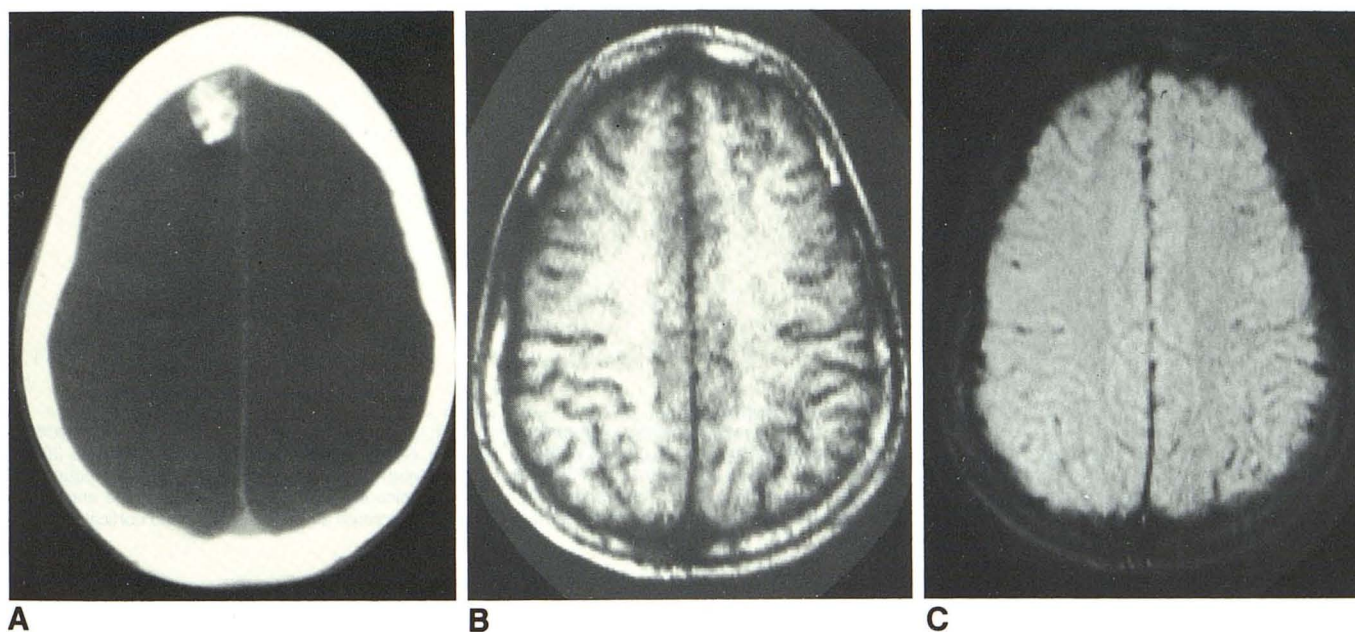


Fig. 5.—(Case 8) Oligoastrocytoma Grade II. **A**, IV contrast-enhanced CT. Densely calcified right frontal mass is readily apparent. **B**, SE 500/30, TR/TE. The extent of abnormality is less on MR image and, prospectively, may not be distinguishable from CSF located deep within a sulcus. **C**, SE 1500/60, TR/TE.

Again, the extent of abnormality is underestimated as the calcified focus shows a signal intensity slightly greater than cortical bone but less than cortical gray matter.

more sensitive than other X-ray-based technologies in detecting calcification [1]. The exact capability of MR, using standard pulse sequences, for reliably predicting the presence of this abnormality has not been sufficiently evaluated. While it is recognized that small punctate calcified foci may escape detection by MR [6, 13, 15, 16], the possibility that larger foci

might escape detection has been infrequently stated [14, 16]. Recently, a number of authors have specifically addressed the imaging of calcification by MR and have noted poor detection. Holland et al. [16], reporting on a group of 50 patients with calcified intracranial lesions detected by CT, found that MR, using a system operating at 0.35 T, raised a

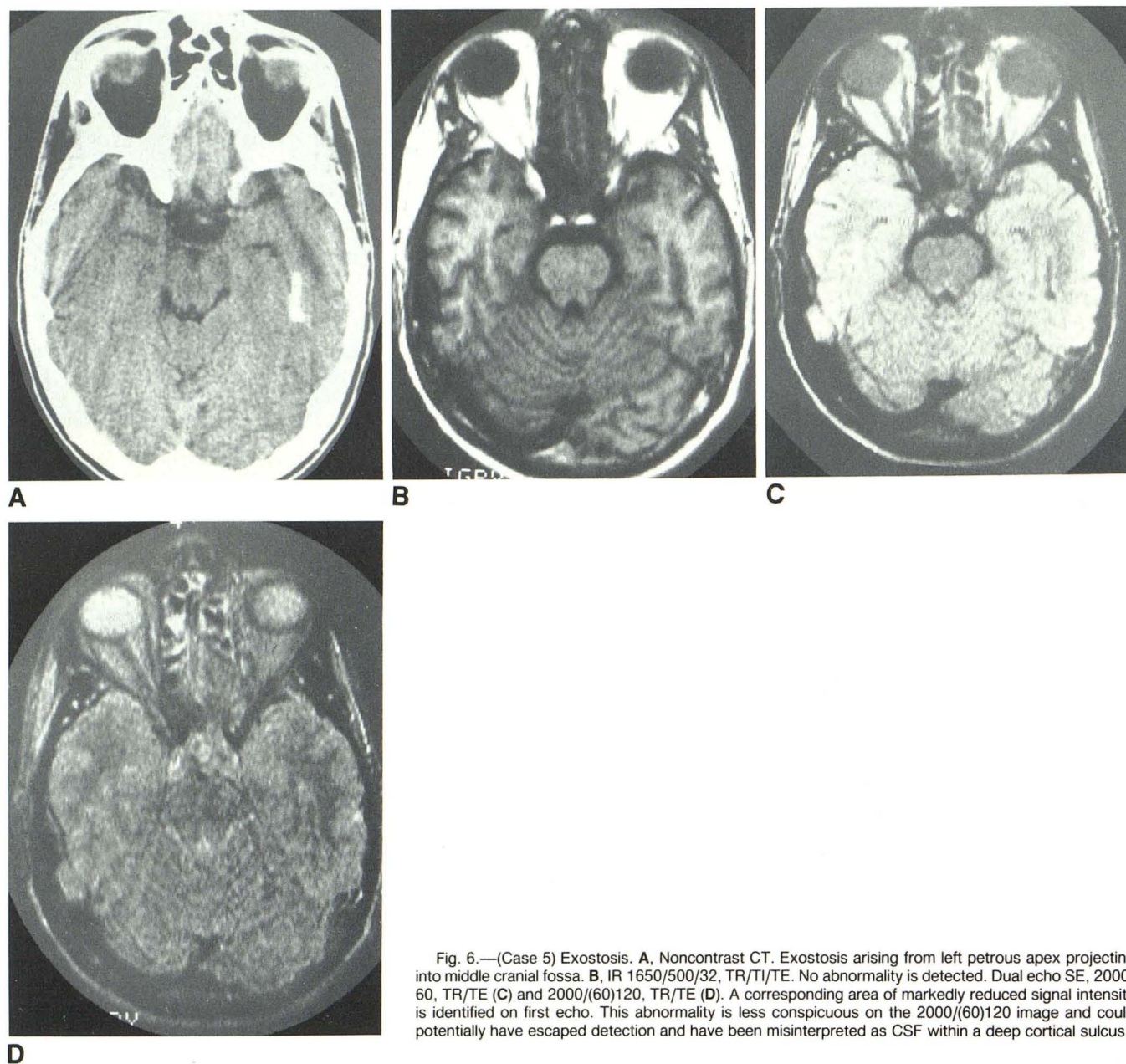


Fig. 6.—(Case 5) Exostosis. **A**, Noncontrast CT. Exostosis arising from left petrous apex projecting into middle cranial fossa. **B**, IR 1650/500/32, TR/TI/TE. No abnormality is detected. Dual echo SE, 2000/60, TR/TE (**C**) and 2000/(60)120, TR/TE (**D**). A corresponding area of markedly reduced signal intensity is identified on first echo. This abnormality is less conspicuous on the 2000/(60)120 image and could potentially have escaped detection and have been misinterpreted as CSF within a deep cortical sulcus.

TABLE 3: Calcification Size vs Detection by MR

Size	Number of Patients	MR Interpretation
Large (>7.5 mm)	8	Definite calcification
		Probable calcification
		Indeterminate
Medium (2.5–7.5 mm)	11	Definite calcification
		Probable calcification
		Indeterminate
Small (<2.5 mm)	1	Definite calcification
		Probable calcification
		Indeterminate

suspicion of the presence of intracranial calcification in approximately 60% of cases. The MR findings were reported to be nonspecific, and the most common finding of calcification was described as a focus of diminished signal rather than signal void. They found that nine of their 50 calcified lesions entirely escaped detection by MR. In a series of meningiomas reported by Zimmerman et al. [12], MR was able to detect calcification in only three of 15 cases in which this finding had been demonstrated by CT. In a series of intracranial vascular malformations, Kucharczyk et al. [13] also reported calcifications to be more reliably detected and characterized by CT and, in their experience, MR completely failed to detect two small calcified lesions that were readily depicted by CT.

In this study, T2-weighted sequences were most sensitive

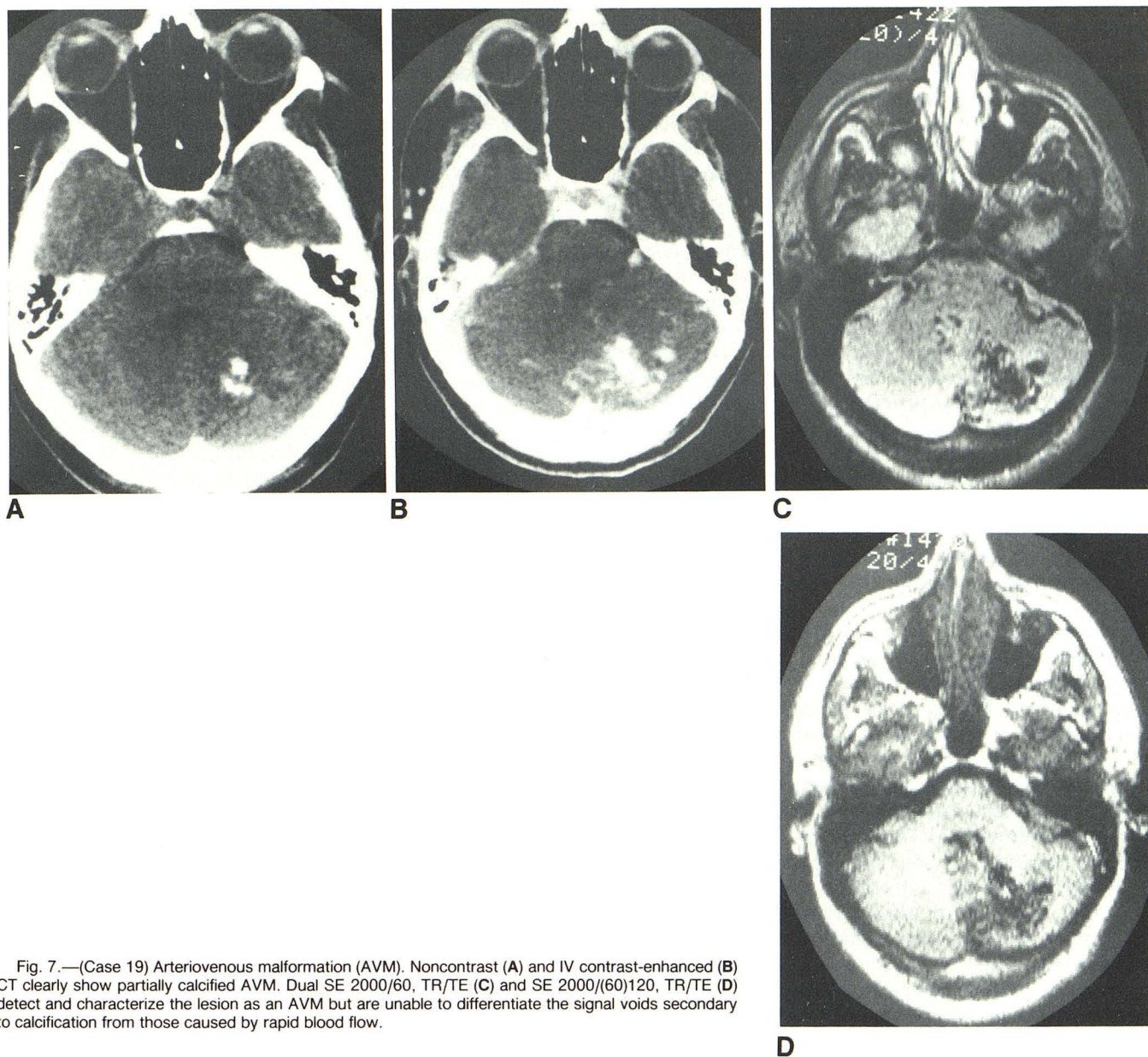


Fig. 7.—(Case 19) Arteriovenous malformation (AVM). Noncontrast (A) and IV contrast-enhanced (B) CT clearly show partially calcified AVM. Dual SE 2000/60, TR/TE (C) and SE 2000/(60)120, TR/TE (D) detect and characterize the lesion as an AVM but are unable to differentiate the signal voids secondary to calcification from those caused by rapid blood flow.

in detecting calcification. This may be explained in part by an increase in conspicuousness of the calcified components of the lesions. Most disease processes in the brain are characterized by prolonged T1 and T2 relaxation constant [20–22]. This leads to their depiction as areas of relative decrease in signal intensity on T1-weighted pulse sequences and as relative increase in signal intensity on T2-weighted pulse sequences. Hence, a reduced signal of calcification within an area of abnormality may be seen with high contrast against the surrounding increased signal on T2-weighted pulse sequences, but may be less conspicuous when surrounded by relatively decreased signal on T1-weighted images. Similarly CSF, having very long T1 and T2 relaxation times [22], will tend to provide higher contrast for some large calcifications

on T2-weighted images compared with T1-weighted images. On the other hand, calcifications that are small compared with the voxel size may be obscured by partial volume averaging with high signal of adjacent soft tissues, especially on T2-weighted images with lower signal to noise ratios [23–25].

The differentiation between the signal void of calcification and that produced by flowing blood may be difficult. The effect of even-echo rephasing of slow intravascular flow may allow for this discrimination in some instances [13, 26–28]. To demonstrate this phenomenon reliably, it may be necessary to use special multiple-echo techniques, such as the five-echo sequence recently reported by Kucharczyk et al. [26]. There is evidence, however, that flow through many normal and abnormal vessels is too rapid to demonstrate this phe-

nomenon. In their series of intracranial vascular malformations, Kucharczyk et al. [13] were unable to demonstrate even-echo enhancement in any instance.

An analysis of the five calcifications in which the signal intensity was profoundly reduced in all available pulse sequences illustrates some of the difficulties inherent to MR in detecting this abnormality. On the basis of the signal intensity characteristics, one would hope that calcification would be highly suspected in each of these instances. In interpreting these cases without knowledge of the CT findings, however, only three lesions were considered to definitely contain calcification. One arteriovenous malformation (AVM) (Fig. 7) was interpreted as being indeterminate, since MR was incapable of distinguishing the signal void of flowing blood from that secondary to calcification in a partially thrombosed AVM. One suprasellar craniopharyngioma (case 15) was judged probably but not definitely to contain calcification. In this case, the signal void of the calcification on the T1-weighted image was of similar signal intensity to adjacent CSF in the suprasellar cistern and hence was inconspicuous. On the T2-weighted image, the signal void of the calcification was seen in higher contrast, but could not definitely be distinguished from the signal void of flow in adjacent major vessels.

The explanation for the variable signal intensity of intracranial calcifications is not entirely clear. In cases in which the abnormality is seen as a signal void, there may be a true paucity of mobile protons, or those present may be behaving in an analogous fashion to the protons present in calcium hydroxyapatite of cortical bone, having extremely prolonged T1 and extremely short T2 relaxation times. It is known that ferromagnetic iron is also present in many calcifications [29]. Ferric iron content could cause a relative signal void by preferential shortening of T2 relaxation [30, 31]. In instances in which calcification is seen as an area of either isointense or slightly reduced signal, there may be a sufficient number of mobile protons in soft tissues within the interstices of the calcification. If a given voxel contains both mobile protons of soft tissue and calcifications, the signal from the mobile protons may predominate and an appreciable signal may be generated. This hypothesis appeared to be supported by one case (case 20) in which we obtained a very heavily proton-density-weighted data set (3500/13, TR/TE). In that patient, the focus of dense calcification was seen as a virtual signal void on the inversion recovery pulse sequence but appeared isosignal with brain on the proton density images.

There are several explanations for the relative superiority of CT in detecting intracranial calcifications. CT is, by its physical nature, exquisitely sensitive to calcium due to both calcium's high density of electrons per unit volume and its marked increase in photoelectric absorption [32, 33]. This is readily reflected as a conspicuous area of higher CT attenuation in the image. The influence of calcifications on the MR image, however, tends to be more subtle. In contrast to CT, where calcification may be positively identified, the presence of this finding can only be inferred through the identification of foci of partial or complete signal dropout in the MR image, which is a nonspecific finding. Holland et al. [16] recently reported that calcification was falsely suspected to be present

in 45% of noncalcified intracranial abnormalities by MR.

To date, the radiologic demonstration of calcification has often added critical information with respect to both the detection and characterization of intracranial lesions. This study demonstrates that MR, operating at 0.6 T and using standard pulse sequences, cannot reliably demonstrate or exclude the presence of calcifications.

REFERENCES

1. Norman D, Diamond C, Boyd D. Relative detectability of intracranial calcifications on computed tomography and skull radiography. *J Comput Assist Tomogr* 1978;2:61-64
2. Bydder GM, Steiner RE, Young IR, et al. Clinical NMR imaging of the brain. *AJNR* 1982;3:459-480, *AJR* 1982;139:215-236
3. Johnson MA, Pennock JM, Bydder GM, et al. Clinical NMR imaging of the brain in children: normal and neurologic disease. *AJNR* 1983;4:1013-1026, *AJR* 1983;141:1005-1018
4. Randell CP, Collins AG, Young IR, et al. Nuclear magnetic resonance imaging of posterior fossa tumors. *AJNR* 1983;4:1027-1034, *AJR* 1983;141:489-496
5. Lee BCP, Kneeland JB, Walker RW, Posner JB, Cahill PT, Deck MDF. MR imaging of brainstem tumors. *AJNR* 1985;6:159-163
6. Brant-Zawadzki M, Davis PL, Crooks LE, et al. NMR demonstration of cerebral abnormalities: comparison with CT. *AJNR* 1983;4:117-124, *AJR* 1983;140:847-854
7. Zimmerman RA, Bilaniuk LT, Goldberg HI, et al. Cerebral NMR imaging: early results with a 0.12 T resistive system. *AJR* 1983;141:1187-1193, *AJNR* 1984;5:1-7
8. Bradley WG Jr, Waluch V, Yadley RA, Wycoff RR. Comparison of CT and MR in 400 patients with suspected disease of the brain and cervical spinal cord. *Radiology* 1984;152:695-702
9. Brant-Zawadzki M, Badami JP, Mills CM, Norman D, Newton TH. Primary intracranial tumor imaging: a comparison of magnetic resonance and CT. *Radiology* 1984;150:435-440
10. Lee BCP, Deck MDF. Sellar and juxtaseellar lesion detection with MR. *Radiology* 1985;157:143-147
11. Sheldon JJ, Siddharthan R, Tobias J, Sheremata WA, Soila K, Viamonte M Jr. MR imaging of multiple sclerosis: comparison with clinical and CT examinations in 47 patients. *AJNR* 1985;6:683-690, *AJR* 1985;145:957-964
12. Zimmerman RD, Fleming CA, Saint-Louis LA, Lee BCP, Manning JJ, Deck MDF. Magnetic resonance imaging of meningiomas. *AJNR* 1985;6:149-157
13. Kucharczyk W, Lemme-Plegghos L, Uske A, Brant-Zawadzki M, Doms G, Norman D. Intracranial vascular malformations: MR and CT imaging. *Radiology* 1985;156:383-389
14. Zimmerman RA. Magnetic resonance imaging of cerebral neoplasms. In: Kressel HY, ed. *Magnetic resonance annual 1985*. New York: Raven Press, 1985:113-145
15. Kjos BO, Brant-Zawadzki M, Kucharczyk W, Kelly WM, Norman D, Newton TH. Cystic intracranial lesions: magnetic resonance imaging. *Radiology* 1985;155:363-369
16. Holland BA, Kucharczyk W, Brant-Zawadzki M, Norman D, Haas DK, Harper PS. MR imaging of calcified intracranial lesions. *Radiology* 1985;157:353-356
17. Taveras JM, Wood EH. *Diagnostic neuroradiology*, 2nd ed. Baltimore: Williams & Wilkins, 1976
18. Newton TH, Potts DG, eds. *Radiology of the skull and brain*. St. Louis: Mosby, 1971
19. Harwood-Nash DC, Fitz CR. *Neuroradiology in infants and children*. St. Louis: Mosby, 1976

20. Brant-Zawadzki M, Bartkowski HM, Ortendahl DA, et al. NMR in experimental cerebral edema: value of T1 and T2 calculations. *AJNR* **1984**;5:125-129
21. Rinck PA, Meindl S, Higer HP, Bieler EU, Pfannenstiel P. Brain tumors: detection and typing by use of CPMG sequences and in vivo T2 measurements. *Radiology* **1985**;157:103-106
22. Beall PT, Amtey SR, Kasturi SR. *NMR data handbook for biomedical applications*. New York: Pergamon Press, **1984**
23. Crooks LE, Hoenninger J, Arakawa M, et al. High-resolution magnetic resonance imaging. *Radiology* **1984**;150:163-171
24. Ortendahl DA, Hylton NM, Kaufman L, Crooks LE. Signal to noise in derived NMR images. *Magn Reson Med* **1984**;1:316-338
25. Edelstein WA, Bottomley PA, Hart HR, Smith LS. Signal, noise, and contrast in nuclear magnetic resonance (NMR) imaging. *J Comput Assist Tomogr* **1983**;7(3):391-401
26. Kucharczyk W, Brant-Zawadzki M, Lemme-Plaghos L, et al. MR technology: effect of even-echo rephasing on calculated T2 values and T2 images. *Radiology* **1985**;157:95-101
27. Bradley WG Jr., Waluch V. Blood flow: magnetic resonance imaging. *Radiology* **1985**;154:443-450
28. Augustyn GT, Scott JA, Olson E, Gilmor RL, Edwards MK. Cerebral venous angiomas: MR imaging. *Radiology* **1985**;156:391-395
29. Lowenthal A, Bruyn GW. Calcification of the striopallidodentate system. In: Vinken PJ, Bruyn GW, eds. *Handbook of clinical neurology*, Vol. 6. Amsterdam: North Holland, **1968**:703-723
30. Wolf GL, Burnett KR, Goldstein EJ, Joseph PM. Contrast agents for magnetic resonance imaging. In: Kressel HY, ed. *Magnetic resonance annual 1985*. New York: Raven Press, **1985**:121-145
31. Stark DD, Moseley ME, Bacon BR, et al. Magnetic resonance imaging and spectroscopy of hepatic iron overload. *Radiology* **1985**;154:137-142
32. Curry TS III, Dowdey JE, Murry RC Jr. *Introduction to the physics of diagnostic radiology*. Philadelphia: Lea and Febiger, **1984**
33. Stanton L. *Basic medical radiation physics*. New York: Appleton-Century-Crofts, **1969**